International Journal of Geography and Geology
2026 Vol. 15, No. 1, pp. 1-18.
ISSN(e): 2305-7041
ISSN(p): 2306-9872
DOI: 10.18488/10.v15i1.4934

Petro-mechanical analysis of rocks near Lake Bosomtwe: Implications for engineering use

Matthew Coffie Wilson[1+]
Emmanuel Mensah[2]
Justice Kwaku Gbemu[3]
Gifty Awuni[4]
Isaac Ayamdoo[5]
Juliet Atta Djabeng[6]

[1,2,3,4,5,6]*Geological Engineering Department, College of Engineering, Kwame Nkrumah University of Science and Technology, Kumasi, Ghana.*
[1]*Email: mcwilson.coe@gmail.com*
[2]*Email: emmanuelmensah6@gmail.com*
[3]*Email: gbemujustice3@gmail.com*
[4]*Email: giftyawuni31@gmail.com*
[5]*Email: ayamdooisaac2@gmail.com*
[6]*Email: jadhielkenzie@gmail.com*


(+ Corresponding author)

Article History
Received: 16 February 2026
Revised: 1 April 2026
Accepted: 10 April 2026
Published: 24 April 2026

Keywords
Abonu
Failure
Lake Bosomtwe
Mechanical analysis
Metasedimentary rocks
Petrography.

ABSTRACT

The main purpose of this project is to determine the petro-mechanical characteristics and their implications for engineering use of rocks near Lake Bosomtwe. The study area is at Abonu near Kuntanase in the Bosomtwe District of the Ashanti Region, Ghana. The study area is underlain largely by Paleoproterozoic rocks (phyllites, metagreywackes) and some Neoproterozoic formations (shale), with the metagreywackes dominating (about 90% of encountered rocks). Petrographic analysis was used to establish the mineralogical, textural, and structural characteristics of the rocks of the study area. An unconfined compressive strength (UCS) measurement was conducted on the sampled rocks using Schmidt Hammer Test and Uniaxial Compressive Strength Test. An Imbibition Method was also used to determine the porosity of some of the sampled rocks. Results of the mechanical strength of the metagreywackes produced unconfined compressive strength values ranging from 18 MPa to 71 MPa, with the metagreywackes showing an inverse relationship with grain sizes. All specimens that were analyzed failed under stress by shattering, except specimen GBOO3B, which failed by shearing along a predefined plane of discontinuity. This form of failure explains that the effects of the identified microstructures are not obvious in the intact rock, a property that makes the rocks suitable as aggregates and engineering materials carrying compressive stresses. The analyzed rocks have effective porosities below 2%, making them suitable for use as concrete, ballasts, and embankment aggregates. However, the high silica content makes the rocks unsuitable for asphalt mixtures due to weak bitumen-silica bonds.

Contribution/Originality: Different textural changes were observed in the metagreywackes, resulting from meteoritic impact in the study area. These metagreywackes exhibited highly fractured and brittle deformation, showed medium UCS, and are better suited for use as aggregates. This phenomenon had never been documented in the study area.

1. INTRODUCTION

1.1. Background of Study

The study area bounded by Lat: 6.528^{0}N - 6.546^{0}N and Long: 1.428^{0}W - 1.445^{0}W, is at Abonu near Kuntanase in Bosomtwe, one of the thirty (30) administrative districts of the Ashanti Region of Ghana. The district is underlain by the Paleoproterozoic and Precambrian basement complex known as Birimian and Tarkwaian formations (GSD-GH, 2023), which lie towards the southeast of the West African Craton. They are about 600 Ma (Black et al., 1979;

Burke & Dewey, 1972). The associated rocks within the study area are predominantly metagreywackes and intercalated phyllite (GSD-GH, 2023).

The Bosomtwe geological setup has attracted significant attention from geology and related fields due to the meteorite impact and its effects on the area's geological formation. Most studies of the Bosomtwe area have focused on petrographic and geochemical analyses of the impact structure (Koeberl, 2005; Osumanu et al., 2024). A notable research effort was a multinational drilling project by the International Continental Scientific Drilling Program (ICDP) in late 2004, during which 16 continuous cores 14 from lake sediments and 2 from impactites were obtained for paleoenvironmental and impact-cratering studies (Karikari, Ferriere, Koeberl, Reimold, & Mader, 2007). Additionally, reports have detailed the petrographic and geochemical characteristics of the main country rock types that likely constituted the target rocks at Bosomtwe, as well as the suevites at the impact structure, including discussions of their pre- and post-impact alteration (Karikari et al., 2007). Our study, however, reports on the petro-mechanics of rocks within the valleys near the Bosomtwe crater and their implications for engineering use.

This study seeks to undertake petrographic analysis through mega- and microscopic observations to determine the mineralogical, textural, and structural relationships. It would also consider the Unconfined Compressive Strength (UCS) test to analyze rock strength.

The mean UCS, an index parameter, a proxy for rock strength which depends on factors such as the loading rate, specimen geometry, specimen size, etc., and its variables are often assumed to represent a reliable rock material property (Bieniawski, 1967). The petrographic and mechanical properties are used to establish suitable engineering use of the rocks. The outcome of this study, therefore, could be used to understand the petro-mechanical properties of the rocks of the study area for engineering purposes.

Petrographic studies provide insight into the evolution of rock suites in an area and the major deformations occurring in the rocks. Strength tests are also relevant in the determination of the mechanical properties, which can be used to classify the rocks in terms of their competence based on the mechanical properties (Wilson, Larbi, Kangah, & Anison, 2022). Understanding the intricate relationship between the petrological characteristics and the mechanical behavior of rocks is crucial for optimizing their utilization in diverse engineering projects and for predicting their response to in-situ stress conditions (Anastasio, Fortes, Kuznetsova, & Danielsen, 2016). The inherent complexities arising from their textural and compositional variability necessitate a comprehensive investigation into their petro-mechanical properties, encompassing strength, deformation, and failure mechanisms (Kalender, Sonmez, Medley, Tunusluoglu, & Kasapoglu, 2014; Thomas, Chin, Pierson, & Sylte, 2003).

The area around Lake Bosomtwe has attracted several studies largely due to the presence of the meteorite impact crater. Although the impact created a large reserve of geologic materials that could serve various engineering purposes, earlier works on the area focused on the impact structure and its immediate environment using petrographic, geochemical, and paleontological analyses to characterize the geological makeup of the terrain (Boateng, Akurugu, Wemegah, & Danuor, 2023; Koeberl, 2005).

The study area is around Lake Bosomtwe, which is approximately 8 kilometers (5 miles) in diameter and is surrounded by steep crater walls.

Figure 1 exhibits the crater walls forming a large reserve of the rocks under study, which can be used as geologic materials for engineering construction purposes. This study provides basic data on the petro-mechanics of the rocks within the study area. This data is necessary for determining the engineering economic potentials of the rocks in the study area. With this information, companies such as quarrying and construction entities can make informed decisions regarding investing in the area.

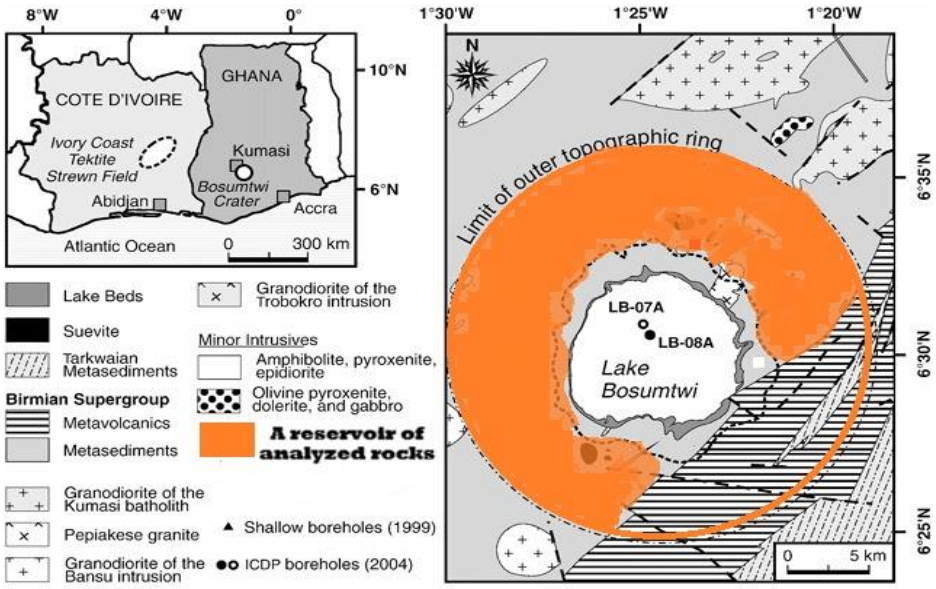

Figure 1. Map of Bosomtwe area showing the reserve of rocks understudied.

The main purpose of this study is to determine the petro-mechanics of the rocks of the study area and their implications for engineering use. The specific objectives to arrive at this main aim are:

To determine the mineralogical, textural, and structural characteristics of the sampled rocks in the study area; to assess the compressive strengths of these rocks, and to evaluate their potential engineering uses based on petro-mechanics.

2. MATERIALS AND METHODOLOGY

2.1. Field Mapping

Before setting off for the field, the topographic map of the study area was acquired from the Ghana Geological Survey Authority in Kumasi to cover the area of interest. Using a GPS device, coordinates were determined for navigation along the chosen traverse and plotting relevant locations, particularly those of samples collected on the base map.

Given the extent of the study area, coupled with the topography, a thorough geological mapping on foot was conducted. The traverses were chosen largely along the terrain where both exposures and sediments within the valleys were mapped. The sediments helped to identify signatures of the various rock types extensively across the higher grounds, making it easier to cover a large area of mapping representatively within the period. GPS coordinates of the areas traversed were taken, as well as those of sampled locations. Attitudes of some geological features (foliation, contacts, faults, joints) were also recorded. Samples were collected from the major lithological units encountered during the mapping. Field descriptions of the rock types were also documented. The rock samples were transported to the Geological and Civil Engineering Laboratories of Kwame Nkrumah University of Science and Technology (KNUST) in Kumasi, Ghana, for petrographic and strength analyses.

2.2. Petrography

2.2.1. Macroscopic Analysis

As part of the petrographic study of the rocks encountered, a detailed description of the mineralogical constituents, texture (grain size, grain shape, sorting of grains), and possible structures was conducted with the aid of a 10x magnifying hand lens. The results were tabulated for further discussion.

2.2.2. Microscopic Analysis

2.2.2.1. Thin Section Preparation

Rocks at the Geological Engineering Laboratory, KNUST, Kumasi, were prepared using a rock cutting machine and labeled. The slabs were cut across and along the layering for each sample. The slabs were gritted with various sizes of gritting papers (60-400) to achieve the desired smoothness. The gritted slabs were bonded onto the frosted surfaces of glass slides using epoxy adhesive. The frosting was done with silicon carbide abrasive powder. The bonded slabs were then trimmed on the glass slides using a trimming machine and further polished on a polishing machine to reduce the thickness of the rock specimens on the slides to a minimum of 30 microns. Figure 2 shows thin sections prepared for petrographic studies. These sections were observed under petrographic microscopes.

Figure 2. Thin sections prepared for petrographic analysis.

2.2.2.2. Observation Under the Microscope

The thin sections of the various samples were observed under petrographic microscopes to establish mineralogical composition, modal estimation, texture, and the presence or absence of microstructures in the sampled rocks.

2.3. Mechanical Analysis

For the purpose of comparison, the Schmidt Hammer test was used to determine the compressive strength of the sampled rocks before the Unconfined Compressive Strength (UCS) test. Figure 3 illustrates an image of a Schmidt Hammer. The UCS, however, was only conducted on two of the samples due to the low level of competence of the

other samples. Both tests were conducted at the Rock Division of the Civil Engineering Department Laboratory of KNUST, Kumasi.

2.3.1. Schmidt Hammer Test

Figure 3. Image of Schmidt hammer.

This is a rebound hammer technique recognized by the American Society for Testing and Materials (ASTM), Deutsche Industrial Norm (DIN), International Organization for Standardization (ISO), etc., as a standard measurement for the compressive strength of engineering materials, particularly concrete and rocks. The Rebound Hammer measures the elastic properties or strength of rocks or concrete, especially their surface hardness and penetration resistance (Wilson et al., 2022). This method was used to determine the compressive strength of all selected samples for analysis.

2.3.2. Coring

Samples were selected carefully to be representative of the original rock formation before coring. Figure 4 illustrates a coring machine on a sampled rock being cored. Two cores, each with a length-to-diameter ratio (L/D) of 2.0, were drilled from the selected samples according to the American Society for Testing and Materials (ASTM) standard. The dimensions used for the cores in the UCS analysis were 45mm in diameter and 90mm in length. It was ensured that the cylindrical surfaces are straight and smooth, with the ends perpendicular during coring and cutting to meet the allowable standards of error margins (deviations not more than 0.02mm and 0.060). Due to the low competence of some rock samples, two (2) out of four (4) selected samples were cored for the UCS test. Figure 5 demonstrates the cored rock samples.

Figure 4. Image of coring machine showing a sampled rock being cored.

Figure 5. Image of cored rock samples.

2.3.3. Uniaxial Test

Figure 6 shows the rock core under UCS. Using the uniaxial compressive stress machine, the maximum compressive strengths of the sampled rocks were determined by subjecting the cored specimens to steadily increasing compressive stresses until failure occurred. Figure 7 demonstrates a failed core under a uniaxial compressive test.

Figure 6. Image of rock core under uniaxial compressive test.

Figure 7. Image of failed core under uniaxial compressive test.

2.3.4. Porosity

For the purpose of assessing the suitability of the sampled rocks for their usage as aggregates, the porosity of two of the sampled rocks were determined (Anastasio et al., 2016) using saturation approach. Figure 8 shows the determination of volume of irregular solids.

Materials

- Geological hammer for breaking the specimens.
- Weighing scale for determining the weight of specimens.
- Measuring cylinder for determining the volumetric measurements.
- Thread for lowering the specimens into the water in the cylinder.
- Oven for drying the specimens.
- Water for saturation and volumetric measurements.

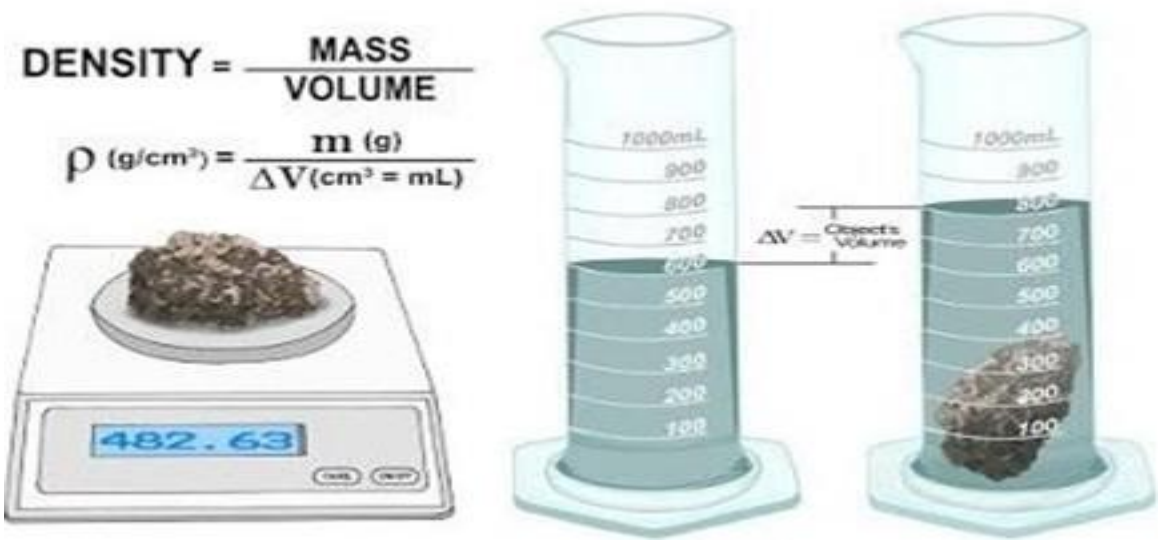

Figure 8. A thematic diagram showing determination of volume of irregular solids.

Procedure: Imbibition Method (Smith & Collis, 1993).

1. Pieces of the rocks were taken and oven dried at 105^{0}C for 24 hours to remove their water content.
2. The masses of these specimens were then determined and recorded as M_D.
3. The specimens were later submerged in water for 48hours to get all available pores saturated.
4. The masses of the saturated specimens were then measured and recorded as M_S.
5. The mass of their respective soaked water, M_W, was determined using the relation, $M_W = M_S - M_D$
6. With the mass of their respective soaked water, we determined the volumes of the soaked water using the density relation, which is equal to the volume of voids, V_V.
7. With a measuring cylinder, we determined the volume of the specimens as V_T.
8. From these parameters (V_T and V_V.), we determined the porosity (n) of the specimens ($n = V_V./ V_T$).

2.3.5. Data Analysis

Results from field and laboratory work were presented in tables, compiled, and plotted into graphs and maps using software such as Microsoft Office Suite, MapInfo, and R-Console. Four samples representing the main lithological units were analyzed. These results form the basis for our discussions.

3. RESULTS AND DISCUSSIONS

3.1. Results

The results presented here are based on the step-by-step observations of the analytical processes undertaken throughout the project. All tests, measurements, and analyses are based on allowable standards and principles within all necessary precautionary frameworks. Figure 9 and Table 1 explain macroscopic or megascopic analyses of specimens of some analyzed rock samples and their mineral constituents.

3.1.1. Petrographic Analysis Results

The petrography encompasses macroscopic and microscopic analyses. The macroscopic analysis involves the use of a hand lens to analyze mineral composition and texture, including grain size, shape, and arrangement. Microscopic petrography involves preparing thin sections of specimens at 30 microns to make them suitable for microscopic analysis.

3.1.1.1. Macroscopic Results

The first phase in petrographic research is macroscopic examination, which offers basic information about the properties of rocks and minerals that may be seen with the unaided eye or with the aid of simple instruments like hand lenses. Classifying geological materials and recognizing characteristics such as texture, grain size, color, and structural orientation requires this method.

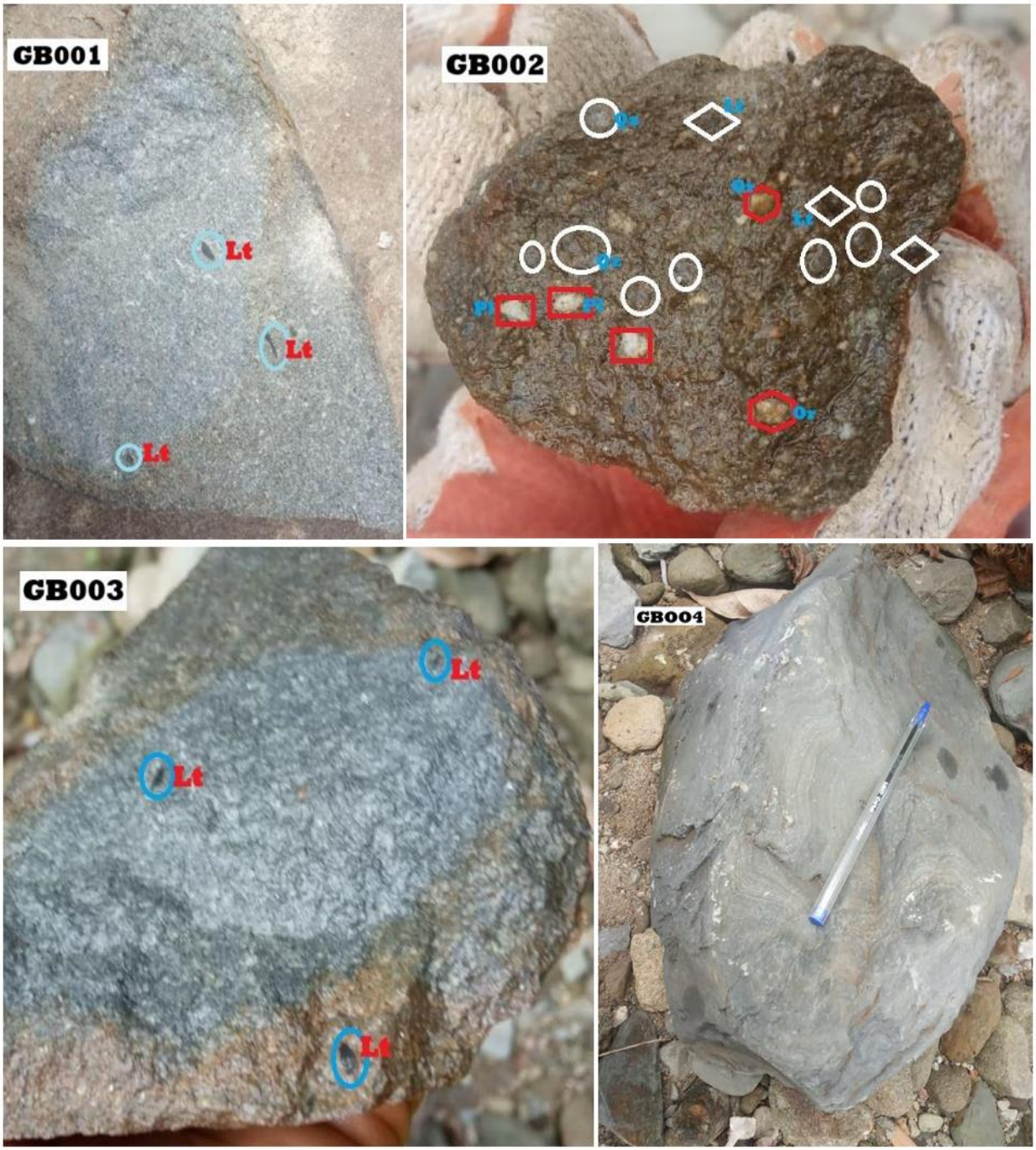

Figure 9. Specimens of rock samples analyzed showing some constituents.

Note: Lt = Lithic mineral/Component; Qz = Quartz; Or = Orthoclase, Pl= Plagioclase.

Table 1. A table of macroscopic descriptions of sampled rocks.

Sample ID	Mineralogy	Texture	Rock type	Others
GB004	Chlorite	Fine-grained, greenish grey	Phyllite	Moderately weathered, layering present, folded, obvious discontinuities
GB003	Muscovite, quartz, feldspar	Medium to coarse grains, angular to sub-rounded grains, fairly sorted, Grey	Metagreywacke	Fresh, minor layering, presence of discontinuities and quartz veins
GB002	Quartz, muscovite, K-feldspar rock fragments.	Coarse grains, poorly sorted, angular to sub-angular grains, yellowish grey	Metagreywacke	moderately weathered, polymictic, presence of quartz veins and fractures
GB001	Muscovite, quartz, feldspar.	Fine to medium grains, angular grains, poorly sorted, Dark grey.	Metagreywacke	Fresh, presence of discontinuities and quartz veins

3.1.1.2. Microscopic Results

Metagreywackes, the predominant rock type of the study area, are often composed of quartz as the key mineral component. Other mineralogical constituents include feldspars (orthoclase and plagioclase), muscovite, opaque minerals, lithic content, and binding material (iron oxide) (Osumanu et al., 2024). The quartz grains appear in two forms. Both types of quartz, monocrystalline and polycrystalline, appear colorless, lack cleavage, and exhibit distinct extinction patterns under microscopic examination, characterized by straight and undulatory (wavy) extinctions, respectively. Quartz (Figure 10) dominates the mineral composition of the metagreywackes, constituting more than 50% of the framework. The quartz grains are typically sub-angular, with monocrystalline quartz being the predominant type, accounting for about 70% of the total quartz content. Figures 10 and 11 and Table 2 demonstrate photomicrographs and modal percentages of metagreywackes samples from Abonu.

Feldspar is the second most abundant observed mineral in the analyzed metagreywackes, with two primary varieties present: orthoclase and plagioclase. Orthoclase appears colorless with two cleavage planes under PPL. It has a distinguishing diagnostic property of Carlsbad twinning or a speckled (dusty) appearance under cross-polarized light (XPL) due to alteration to sericite. The grains have sub-angular to sub-rounded morphology. The orthoclase appeared colorless with two cleavage planes under plane-polarized light (PPL). Fresh plagioclase grains under XPL exhibit well-preserved polysynthetic twinning, characterized by parallel compositional planes. Plagioclases are the predominant feldspar in the metagreywacke samples, with sub-angular to sub-rounded grain shape. Some of the plagioclase grains occur as large, distinctive phenoclasts. In plane polarized light (PPL), muscovite appears colorless, as flakes with platy habits and distinct cleavage. It shows straight extinction under XPL on stage rotation. Opaque minerals in the rock are dispersed and exhibit sub-angular to sub-rounded shapes. Under both PPL and XPL, these minerals consistently appear dark and remain unaffected by stage rotation due to their ability to block transmitted light. Iron oxides are present in the greywacke as a cementing agent, characterized by a greyish-brown coloration that typically accumulates along mineral boundaries. This discoloration likely results from water or moisture reacting with the edges of loosely packed grains, promoting oxide formation. The iron oxide often forms an interconnecting network around quartz grains.

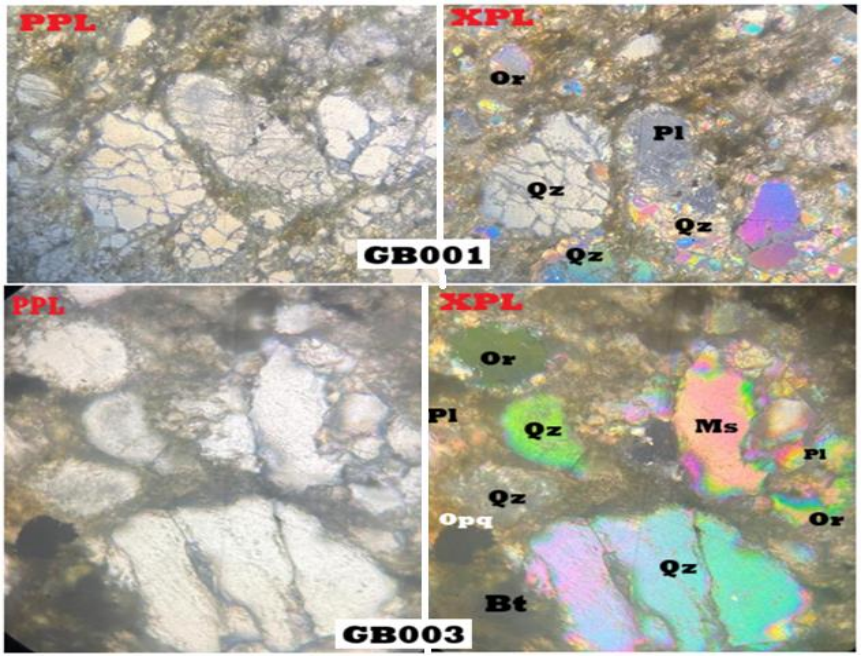

Figure 10. Photomicrographs of parallel thin-sections of rock samples GB001 and GB003 showing some minerals under both PPL and XPL.

Note: Lt = lithic mineral/component; Qz = quartz; Or = orthoclase, Pl = plagioclase, Opq = opaque minerals, Ms = muscovite, Bt biotite.

Table 2. Table of modal estimation of the metagreywackes.

Sample ID	Qz%	Or%	Pl%	Ms%	Bt%	Lt%	Others%	QFL		
								Qz%	F%	Lt%
GB001	60	3	5	10	3	1.5	17.5	86	12	2
GB002	50	6	9	15	6	4	10	72	22	6
GB003	55	5	7	12	5	2	14	80	17	3

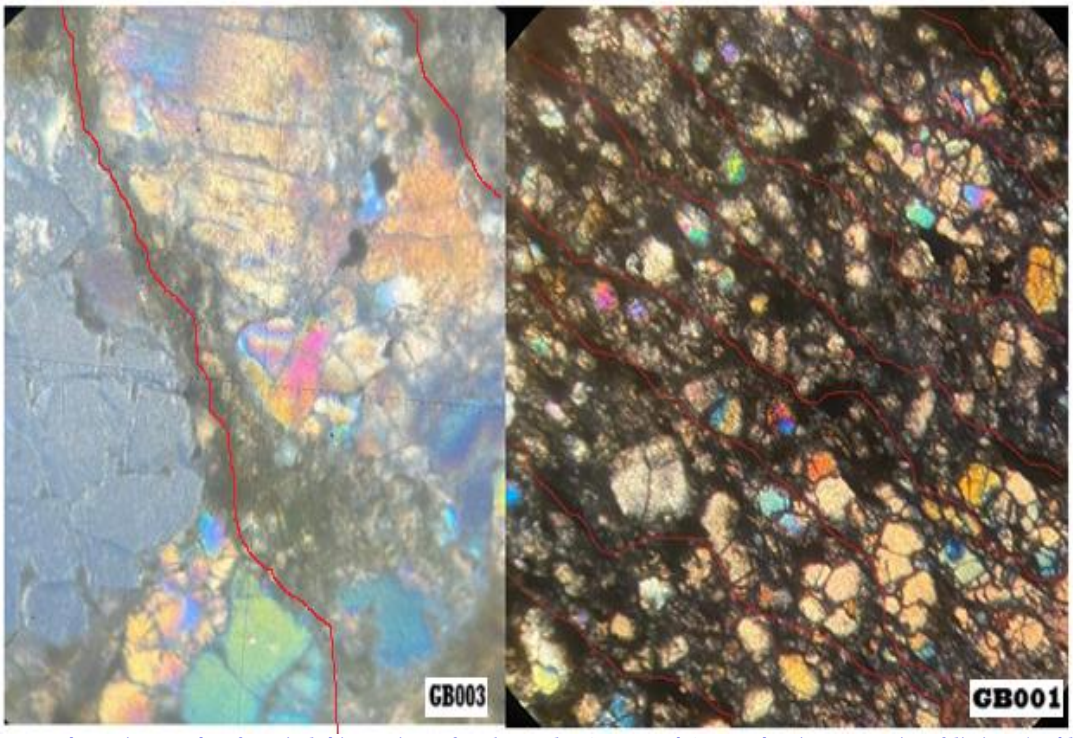

Figure 11. Photomicrographs of vertical thin-sections of rock samples GB001 and GB003 showing some micro foliations (Red lines).

3.1.2. Mechanical Analysis Results

The mechanical analysis of the rock samples comprises unconfined compressive strength (UCS) and Schmidt Hammer tests. This is done to exhibit the strengths of the rocks in the study area.

3.1.2.1. Schmidt-Hammer Results

The Schmidt Hammer test is helpful for estimating the compressive strength of rock specimens. This test is a non-destructive method for analyzing rock strength. Table 3 presents the results of sampled rocks using the Schmidt Hammer.

Table 3. Table of Schmidt hammer results of sampled rocks.

Sample ID	Test 1	Test 2	Test 3	Average	Rock type
GB001	64 MPa	70 MPa	64 MPa	66 MPa	Fine to medium-grained metagreywacke
GB002	27 MPa	14 MPa	14 MPa	18.33 MPa	Coarse-grained polymictic metagreywacke
GB003	54 MPa	47 MPa	47 MPa	49.33 MPa	Medium to coarse-grained metagreywacke
GB004	28 MPa	16 MPa	21 MPa	21.67 MPa	Phyllite

3.1.2.2. Unconfined Compressive Strength (UCS) Results

The mechanical properties of Birimian rocks, such as UCS values and rock competence, are essential for engineering applications. The mechanical strength of Birimian rocks is a critical parameter for engineering applications. The UCS values for Birimian rocks vary significantly depending on lithology. Figures 12 and 13 present the outcomes and graphs of the UCS values of the rock samples, exhibiting their rock textures (fine- to coarse-grained). Table 4 also presents the UCS values of the rock specimens. Moreover, Table 5 is constructed to present the classification of the strengths or hardness of the various rocks in the study area.

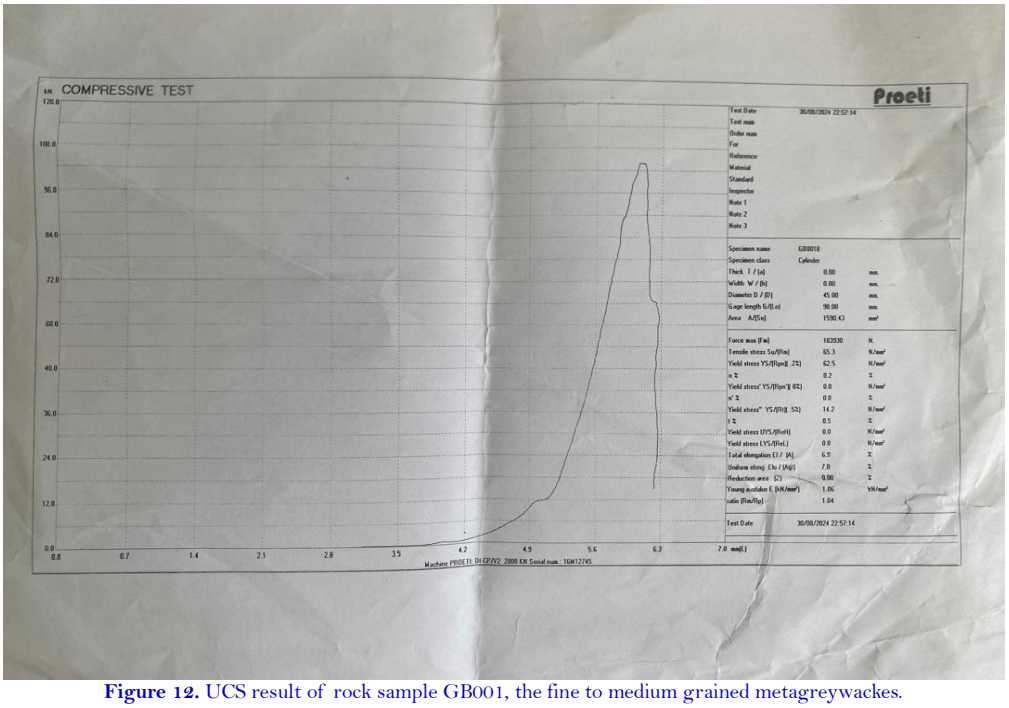

Figure 12. UCS result of rock sample GB001, the fine to medium grained metagreywackes.

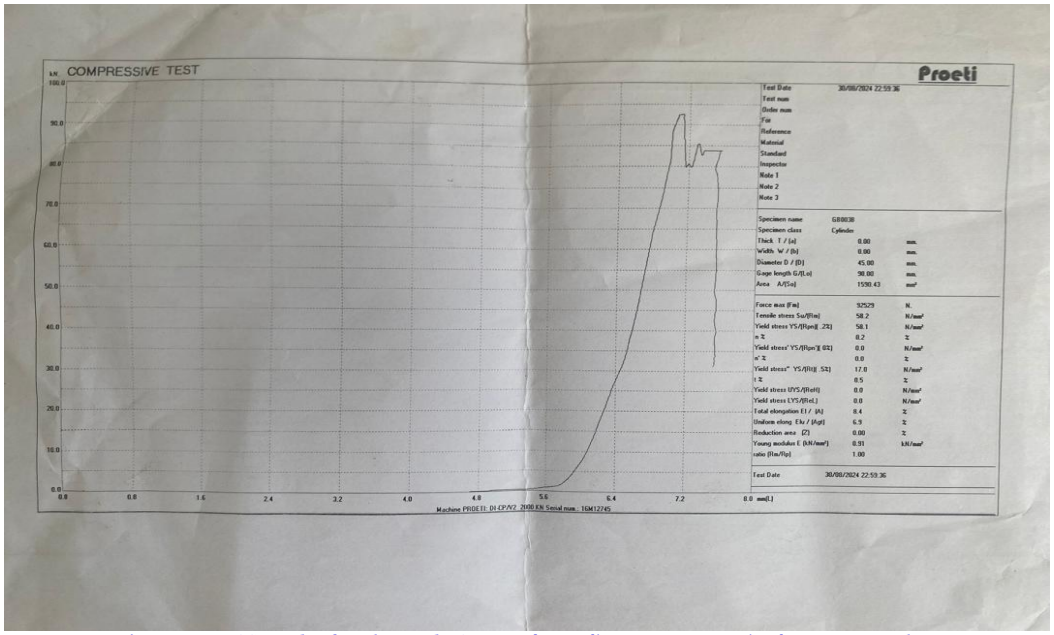

Figure 13. UCS result of rock sample GB003, the medium to coarse grained metagreywackes.

Table 4. Table of UCS results of rock specimens.

Core Diameter, D	45 mm			
Core Length, L	90 mm			
Cross-Sectional Area	1590.43 mm²			
Sample ID	**UCS (MPa)**	**Max Load (KN)**	**Young Modulus, E (KN\mm²)**	**Rock Type**
GB001A	67.40	107.30	3.05	Fine to medium-grained metagreywacke
GB003A	65.30	103.90	1.06	Medium to coarse-grained metagreywackes
GB001B	71.00	112.90	0.50	Fine to medium-grained metagreywackes
GB003B	58.20	92.30	0.91	Medium to coarse-grained metagreywacke

Table 5. Classification of rock hardness (Attewell & Farmer, 1976).

Strength Classification	Strength Range (MPa)	Typical Rock Types
Very weak	10-20	Weathered and weakly compacted sedimentary rocks
Weak	20-40	Weakly-cemented sedimentary rocks, schists
Medium	40-80	Competent sedimentary rocks; some low-density coarse-grained igneous rocks
Strong	80-160	Competent igneous rocks, some metamorphic rocks, and fine-grained sandstones

3.1.2.3. Porosity

Porosity explains the measure of void spaces in the rock specimen. Porosity, permeability, and the measure of the pores in the rock specimen, as well as how connected they are to one another. The ease with which fluids flow through the rock specimen is very important. Table 6 presents measurements of the masses of some rock specimens, whilst Table 7 presents the volumetric measurements of some of the rock specimens.

Table 6. Table of measurements of masses of rock specimens.

Sample Id	Dry Mass (g)	Saturated Mass (g)	Mass of soaked water (g)
GB001B	269.20	270.40	1.20
GB001B	176.60	177.80	1.20

Computations:

GB001B => Volume (H_2O) = Volume of voids (V_V) = Mass of H_2O(M_W) / Density of H_2O

$V_V = 1.2/1 = 1.2\ cm^3$

GB003B => Volume (H_2O) = Volume of voids (V_V) = Mass of H_2O(M_W) / Density of H_2O

$V_V = 1.2/1 = 1.2\ cm^3$

Table 7. Table of volumetric measurements of rock specimens.

Sample ID	Initial H_2O level in cylinder, V_1 (cm^3)	H_2O level after submersion, V_2 (cm^3)	Volume of specimen, V_2 - V_1 (cm^3)
GB001B	950.00	1017.40	67.40
GB003B	1011.40	1111.60	100.20

Computations:

GB001B => Volume of specimen, $V_T = 67.40cm^3$

- Porosity, $n = V_V / V_T = 1.2 / 67.4 = 0.018 = 1.8\%$

GB003B => Volume of specimen, $V_T = 100.20cm^3$

- Porosity, $n = V_V / V_T = 1.2 / 100.2 = 0.012 = 1.2\%$

3.2. Discussions

3.2.1. Geologic Setting of the Study Area

The rocks encountered within the study area are primarily of Paleoproterozoic age (metagreywackes and phyllites), with a rare, highly weathered shale formation that appears to be of Neoproterozoic age. The metagreywackes dominate, covering about 90% of the encountered rocks. There are varieties of metagreywackes ranging from fine-medium grained, medium-coarse grained, to coarse-polymictic grained in the terrain. They have been subjected to severe brittle deformation, evident in the high level of fracturing within the terrain. Weathering is prevalent in the coarse-polymictic metagreywackes compared to other varieties. The minority phyllites appear sandwiched between blocks of metagreywackes in most cases. They have suffered both brittle and elastic deformations and appear moderately to highly weathered. Figure 14 represents a highly weathered shale at the study area.

Figure 14. A highly weathered shaly formation near the outskirts of the topographic ring within the study area.

The protolith greywacke, characterized by a predominance of quartz along with orthoclase and plagioclase, indicates a sedimentary origin of these rocks (Osumanu et al., 2024). It responded to tectonic activity in a brittle manner, registering fractures intruded by residual magma, which left traces of quartz veins oriented haphazardly throughout the terrain. This new lithology was further subjected to brittle deformation, creating apertures that were subsequently filled during the deposition of clay materials, lithified into shales sandwiched between blocks of

metagreywackes. Later intense tectonic activity caused the shales to metamorphose into phyllites, folding and fracturing them in the process. The metagreywackes were further crystallized into higher-grade metagreywackes, with intensity decreasing away from the crater's core, which could easily be mistaken for igneous rock at a glance.

This crystallinity, however, did not come without appreciable brittle deformation evident in the highly fractured rocks with shear and fault zones. This chronology of events is arrived at because thin beds of the phyllites are found sandwiched between blocks of the metagreywackes, and the quartz veins (intrusions) are only found in the metagreywackes but not in the phyllites. Figures 15 and 16. represent field pictures of metagreywackes sandwiching phyllite and metagreywackes intruded by quartz.

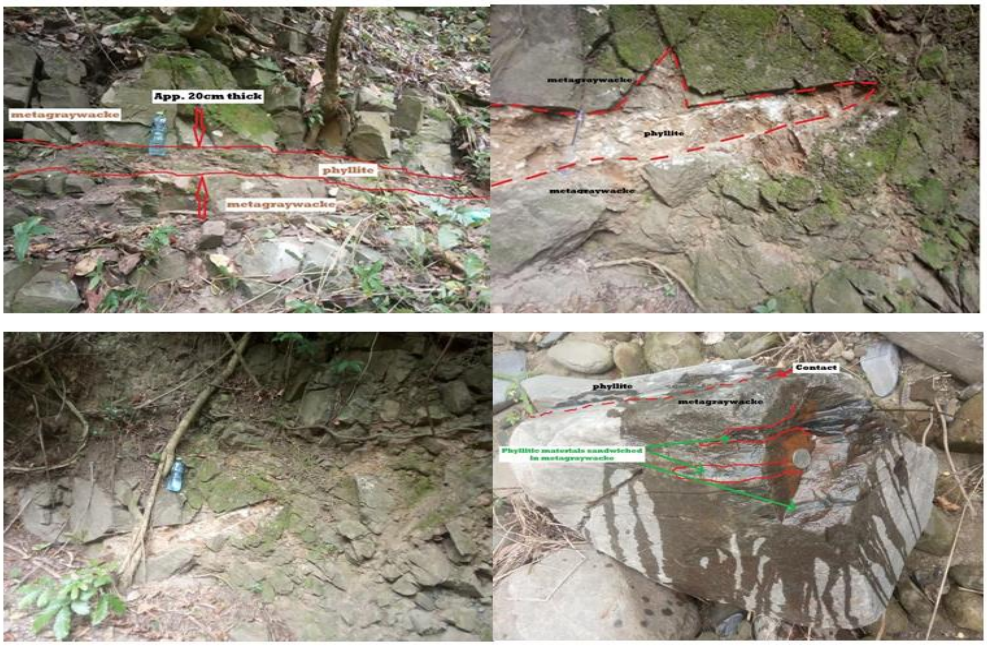

Figure 15. Field pictures showing phyllitic materials sandwiched within blocks of metagreywackes at the study area.

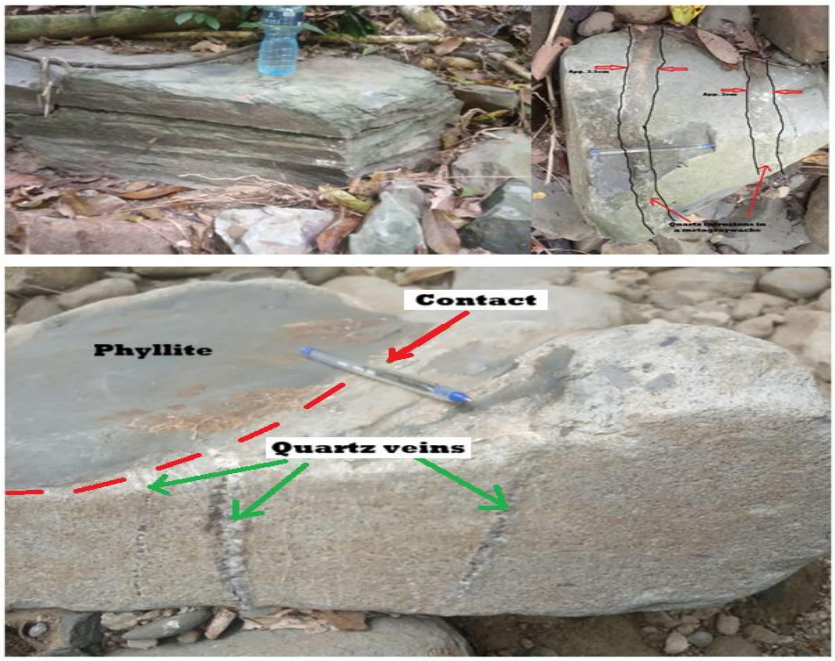

Figure 16. Field pictures showing quartz veins within metagreywacke but not in phyllites at the study area.

3.2.2. Petro-Mechanics

3.2.2.1. Petrographic Consideration

According to Osumanu et al. (2024), which has been largely ascertained by this study, the metagreywackes of Bosomtwe are mainly composed of quartz (mostly monocrystalline), feldspars, micas, lithic fragments, and some opaque minerals. Observation and analysis have shown that the rudaceous (coarser) metagreywackes with higher lithic, feldspathic, and micaceous proportions, versus lower quartz proportion, are highly susceptible to chemical weathering, making them unsuitable for engineering use. It was also observed that the mechanical strength of the metagreywackes has an inverse relationship with grain size, given that the analyzed samples have similar cementing material, grain angularity, and mineralogical composition. Microscopic observations reveal some weak internal foliation in the vertical thin sections.

Silica minerals usually cause low adhesion between the binding material and aggregates in asphalt mixtures, negatively affecting pavement durability (Anastasio, 2015). For this reason, the high quartz proportion in metagreywacke makes it unsuitable for use as aggregates in asphalt mixtures

Pore sizes smaller than 5 microns in diameter negatively affect the durability of rock materials due to slow fluid circulation inside the rock, which increases the effects of damaging processes such as freeze-thaw (Fort, Varas, Alvarez de Buergo, & Martin-Freire, 2011; Russel, 1927). Although recrystallization has reduced pore sizes in metagreywackes (actual sizes not measured in this study), the tropical setting in Ghana prevents freeze-thaw processes, eliminating this threat. Combined with the weathering-resistant mineralogical composition and medium compressive strength, these properties make metagreywackes suitable for use as road and rail ballasts.

3.2.2.2. Failure Type

Apart from specimen GBOO3B, which failed by shearing along a predefined zone of discontinuity and attained a UCS value of 58.2 MPa, the specimens analyzed failed under stress by shattering. This form of failure indicates that the effects of properly defined microstructures are absent in the intact rock, a property that makes rocks suitable as aggregates and engineering materials capable of bearing compressive stresses. When crushed, these rocks produce highly spherical and angular shapes. Elongated and/or flaky shapes of crushed aggregates can negatively affect their use as road material, coarse concrete aggregate, and ballast for railways. Such shapes decrease the mechanical resistance of the material, impacting the stability of railway structures or road surface layers, and reduce workability for fresh concrete(Wnek, Tutumluer, Moaveni, & Gehringer, 2013). Figure 17 demonstrates core specimens that have shown failure under compressive stress.

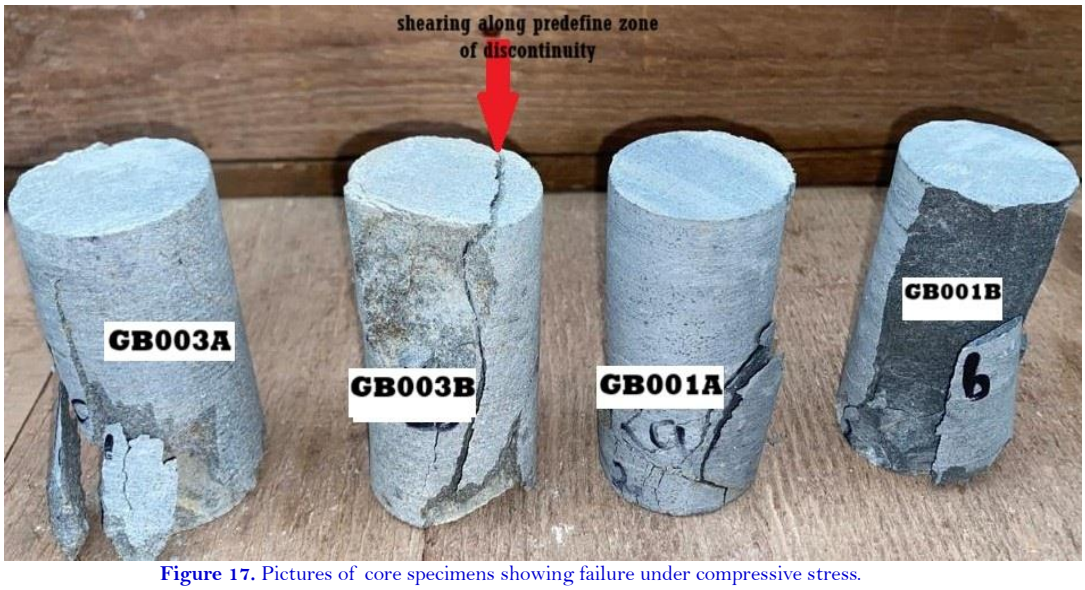

Figure 17. Pictures of core specimens showing failure under compressive stress.

4. CONCLUSIONS

Based on the outcome of the analysis and observations made during this project, the following deductions are made.

4.1. Petrography

The predominant rock type within the study area is metagreywackes. On a large scale, they are highly fractured, depicting brittle deformation. They contain quartz veins and are slightly weathered, with weak to no visible layering. These rocks have a high quartz proportion, low lithic content, and average mica and feldspar composition. They have angular, medium to coarse grains with micro-foliation and an average effective porosity of less than 2%. The next abundant rock type in the terrain is the phyllites. They are folded and fractured, evidence of both ductile and brittle deformations, moderately to highly weathered, and foliated. They are fine-grained with a pale green coloration, indicating chlorite content, suggesting greenschist-facies. The other minor lithology encountered appears to be a Neoproterozoic rock (shale). This unit is highly weathered, showing horizontal bedding with very thin beds in some cases.

4.2. Mechanics

The phyllite recorded a weak UCS average of 21.67 MPa. The metagreywacke recorded a medium UCS average of 60.2 MPa. The metagreywackes analyzed using UCS test failed under stress due to shattering. They are also resistant to weathering.

4.3. Engineering Usage

The measured UCS average, together with the failure characteristic, makes the metagreywackes suitable for use as aggregates. Failing by shattering implies a relatively more spherical and angular aggregate when crushed. This increases the mechanical resistance of the material, positively affecting their stability under load (Wnek et al., 2013). Also, the effective porosity of less than 2% qualifies these aggregates for concrete works. The aggregates, however, are unsuitable for use as aggregates in asphalt mixtures due to the high quartz proportion of the metagreywacke. This is because silica-bitumen bonds are generally weak, reducing the strength of the asphalt pavement surface (Anastasio, 2015). On the other hand, the high quartz component, coupled with the moderate estimated UCS average, implies resistance to weathering and compressive load, making the metagreywackes ideal for use as road and railway ballasts, embankments (dams, roads, slope support, etc.), ripraps, sea defense walls, etc.

The foliation could generate elongated and flaky particles when crushed, making the possible use of phyllite not suitable for concrete as well as ballast material. The elongated aggregates could easily crack when supporting high loads, such as in concrete constructions or passing trains, resulting in dangerous situations. This was recorded in 1963 in Zamora (Spain), where a dam failure was caused by the use of schist aggregates (Torroja & Torroja, 1963).

Funding: This research was funded by the individual Authors.
Institutional Review Board Statement: Not applicable.
Transparency: The Authors state that the manuscript is honest, truthful, and transparent, that no key aspects of the investigation have been omitted, and that any differences from the study as planned have been clarified. This study followed all writing ethics.
Competing Interests: The Authors declare that they have no competing interests.
Authors' Contributions: All Authors contributed equally to the conception and design of the study. All Authors have read and agreed to the published version of the manuscript.

REFERENCES

Anastasio, S. (2015). *Evaluation of the effect of aggregate mineralogy on the durability of asphalt pavements.* Trondheim: Department of Civil and Transport Engineering, Norwegian University of Science and Technology.

Anastasio, S., Fortes, A. P. P., Kuznetsova, E., & Danielsen, S. W. (2016). Relevant petrological properties and their repercussions on the final use of aggregates. *Energy Procedia*, *97*, 546-553. https://doi.org/10.1016/j.egypro.2016.10.073

Attewell, P. B., & Farmer, I. W. (1976). *Principles of engineering geology*. London: Chapman and Hall.

Bieniawski, Z. T. (1967). Mechanism of brittle fracture of rock: Part I—theory of the fracture process. *International Journal of Rock Mechanics and Mining Sciences & Geomechanics Abstracts*, *4*(4), 395-406. https://doi.org/10.1016/0148-9062(67)90030-7

Black, R., Caby, R., Moussine-Pouchkine, A., Bayer, R., Bertrand, J. M., Boullier, A. M., . . . Lesquer, A. (1979). Evidence for late Precambrian plate tectonics in West Africa. *Nature*, *278*(5701), 223-227. https://doi.org/10.1038/278223a0

Boateng, C. D., Akurugu, C. A., Wemegah, D. D., & Danuor, S. K. (2023). Underrepresentation of local researchers in geophysical studies at the Bosumtwi impact crater: Insights from a systematic review. *Scientific African*, *21*, e01893. https://doi.org/10.1016/j.sciaf.2023.e01893

Burke, K. C., & Dewey, J. F. (1972). Orogeny in Africa: African geology. In (pp. 583-608). Ibadan: Ibadan University Press.

Fort, R., Varas, M. J., Alvarez de Buergo, M., & Martin-Freire, D. (2011). Determination of anisotropy to enhance the durability of natural stone. *Journal of Geophysics and Engineering*, *8*(3), S132-S144. https://doi.org/10.1088/1742-2132/8/3/S13

GSD-GH, G. S. D. (2023). *Geology of Bosomtwe*. Ghana: Bosomtwe District. S.N.

Kalender, A., Sonmez, H., Medley, E., Tunusluoglu, C., & Kasapoglu, K. (2014). An approach to predicting the overall strengths of unwelded bimrocks and bimsoils. *Engineering Geology*, *183*, 65-79. https://doi.org/10.1016/j.enggeo.2014.10.007

Karikari, F., Ferriere, L., Koeberl, C., Reimold, W. U., & Mader, D. (2007). Petrography, geochemistry, and alteration of country rocks from the Bosumtwi impact structure, Ghana. *Meteoritics & Planetary Science*, *42*(4-5), 513-540. https://doi.org/10.1111/j.1945-5100.2007.tb01058.x

Koeberl, C. (2005). Bosumtwi impact crater, Ghana (West Africa): An updated and revised geological map, with explanations. *Yearbook of the Geological Survey of Austria*, *145*(1), 1-31.

Osumanu, J., Brako, B., Yalley, O. K., Adams, A. R., Appiah, D., & Aminu, M. B. (2024). Mineralogical characteristics of greywackes at Lake Bosomtwe Area in the Ashanti Region of Ghana. *European Journal of Environment and Earth Sciences*, *5*(2), 23–30. https://doi.org/10.24018/ejgeo.2024.5.2.449

Russel, S. A. (1927). *Stone preservation committee report (Appendix I)*. London: H.M. Stationary Office.

Smith, M. R., & Collis, L. (1993). *Aggregates: Sand, gravel and crushed rock aggregates for construction purposes* (2nd ed.). London: Geological Society of London.

Thomas, L. K., Chin, L. Y., Pierson, R. G., & Sylte, J. E. (2003). Coupled geomechanics and reservoir simulation. *SPE Journal*, *8*(4), 350-358. https://doi.org/10.2118/87339-PA

Torroja, M. E., & Torroja, C. J. A. (1963). *Technical reports and judicial sentence on the rupture of the Vega de Tera Dam in Ribadelago Galende (Zamora)*. Madrid, Spain: Institute of Engineering of Spain.

Wilson, M. C., Larbi, J., Kangah, I. I., & Anison, E. (2022). Petro-mechanical studies of the stratigraphic units of the Tarkwaian Supergroup in Tarkwa – Implications for the structural and mechanical competence of rocks. *Malaysian Journal of Geosciences*, *6*(1), 1-7. https://doi.org/10.26480/mjg.01.2022.01.07

Wnek, M. A., Tutumluer, E., Moaveni, M., & Gehringer, E. (2013). Investigation of aggregate properties influencing railroad ballast performance. *Transportation Research Record: Journal of the Transportation Research Board*, *2374*(1), 180-189. https://doi.org/10.3141/2374-21